Turnitin artikel bu Lidya

by alfonsus oki

Submission date: 02-Feb-2024 02:11PM (UTC+0700)
Submission ID: 2214809094
File name: artikel_bu_Lydia.pdf (4.56M)
Word count: 7766
Character count: 40729

Research Article

Mohamad Irfan Fathurrohman*, Santi Puspitasari, Asron Ferdian Falaah, Lydia Anggraini, Nanang Ali Sutisna, and Rijal Hakiki

Utilization of biosilica for energy-saving tire compounds: Enhancing performance and efficiency

https://doi.org/10.1515/epoly-2023-0043
received May 03, 2023; accepted August 15, 2023

Abstract: Energy-saving tires have been developed by researchers in the industry in order to minimize hysteresis loss. In general, this is achieved by combining precipitated silica sourced from silica sand with a silane coupling agent. This strategic reaction serves to elevate the performance characteristics of tread tire, effectively enhancing their properties. Therefore, this research is aimed to investigate the utilization of commercially available biosilica compared to high dispersed (HD) silica, examining their potential as reinforcing agents in the composition of passenger tread tire compound. This compound was formulated using a blend of solution styrene-butadiene rubber (SSBR) and butadiene rubber (BR). A comprehensive analysis was conducted to assess the impact of varying ratios between biosilica and HD silica on the mechanical and dynamic properties of tread tire compound composed of SSBR and BR blend. The results showed that the incorporation of biosilica could effectively reduce the filler network resulting in better dispersion of biosilica in the SSBR/BR blend matrix. As a result, it improved wet grip (44%) and rolling resistance (26%) while maintaining abrasion resistance compared with HD silica in passenger tread tire compound. The application of biosilica as an eco-friendly reinforcement material exhibited its potential for elevating the performance of energy-efficient tread tire.

* **Corresponding author: Mohamad Irfan Fathurrohman**, Bogor Getas Research Unit, Indonesian Rubber Research Institute, 1 Salak Rd, Bogor, West Java 16128, Indonesia, e-mail: irfanirri@gmail.com
Santi Puspitasari: Bogor Getas Research Unit, Indonesian Rubber Research Institute, 1 Salak Rd, Bogor, West Java 16128, Indonesia, e-mail: santi.puspitasari.ppk@gmail.com
Asron Ferdian Falaah: Bogor Getas Research Unit, Indonesian Rubber Research Institute, 1 Salak Rd, Bogor, West Java 16128, Indonesia
Lydia Anggraini, Nanang Ali Sutisna: Department of Mechanical Engineering, President University, Bekasi, West Java 17530, Indonesia
Rijal Hakiki: Department of Environmental Engineering, President University, Bekasi, West Java 17530, Indonesia

Keywords: high dispersed silica, biosilica, passenger tread tire, energy-saving tire, tire labeling

1 Introduction

Tire labeling regulation is mandatory for all tire commercialization within the European Union territory. The first implementation of this regulation was in 2012 and was introduced only for car and van tires. Subsequently, the most recent iteration of these rules, effective since May 2021, extended the labeling requirement to include tires for buses and lorries. This labeling provides essential information primarily about the safety and environmental performance of a new tire including fuel efficiency, noise, and wet grip, which is known as the magic triangle. The fuel consumption of a car is highly affected by tread tire rolling resistance. Therefore, tire industries worldwide compete to develop new tread tire formulations based on regulation and labeling.

The efficiency of a car's fuel consumption is significantly influenced by the tread design of the tires, which plays a crucial role in optimizing the vehicle's movement. A new silica-silane system was introduced by Michelin to replace carbon as a reinforcing filler in the rubber compound. The aim of this invention was to improve the tire's rolling resistance and wet grip (1,2). The high concentration of silanol groups on the silica surfaces encounter difficulties in dispersing silica, specifically in non-polar rubber commonly used for rubber tread compound such as styrene-butadiene rubber or butadiene rubber (BR). The incorporation of silane as a coupling agent (such as bis (triethoxysilylpropyl) tetrasulfide; TESPT) into silica-filled rubber systems improves compatibility between silica and non-polar rubber due to physical and chemical interaction through a process known as silanization reaction. The silanol groups on the silica surface chemically interact with ethoxy groups in TESPT molecules. Furthermore, the polysulfide within

TESPT molecules chemically interacts with rubber molecules during vulcanization, leading to improvement in rubber–silica interaction (3).

Silica industries developed new types, specifically for producing low rolling resistance tire (energy-saving tire), called high dispersed (HD) silica. Subsequently, HD silica is characterized by a high specific surface area (SSA). Nowadays, this new type of silica consumption has increased with the raising demand for energy-saving tire in the market. Other alternatives for silica sources include renewable resources, such as rice husk, palm oil fuel ash, sugarcane bagasse ash, and bamboo leaf ash (4). Among these, rice husk showed higher silica content of approximately 90%, compared to others (5), making it a potential raw material for producing biosilica used as reinforcing filler in the tire industry (6).

Researchers use various methods to produce biosilica from rice husk, using several mechanisms. These processes involve hydrothermal, thermo-chemical, chemical, and biological or a combination of thermochemical and chemical processes (7). The chemical process is important to enhance the surface area of biosilica since it strongly affects the reinforcement of rubber. The surface area and purity of biosilica from rice husk can be increased by acid leaching using HCl or H_2SO_4. The obtained surface area of biosilica was 218 and 208 $m^2 \cdot g^{-1}$ by using HCl and H_2SO_4 for acid leaching, respectively (7). Arayapranee et al. (8) conducted a comparative analysis involving fillers of varying surface areas. The research found that rice husk ash with a lower surface area showed poor abrasion resistance, rendering it unsuitable for rubber tread compound. There exists a pressing need to elevate the surface area of rice husk biosilica to a level around 104 $m^2 \cdot g^{-1}$, similar to that of conventional silica of 112 $m^2 \cdot g^{-1}$. The abrasion resistance of tire tread from rice husk biosilica equal to conventional silica (6).

Another important property of amorphous silica is the presence of silanol groups attached to the silica surfaces. The identification of these existing silanol groups can be achieved through Fourier transform infra-red (FTIR) analysis. Subsequently, FTIR spectra showed that silanol groups were exhibited at the broad absorption band at 3,200–3,750 cm^{-1}. The range of wavenumbers was attributed to the silanol groups and interaction between water and adjacent (vicinal) silanols (6,9). In addition, asymmetric stretching vibration of Si–O on Si–OH at 940–960 cm^{-1} indicated the presence of silanol groups on the silica surfaces (10). Silanol groups present on the silica surface act as functional groups capable of undergoing chemical reactions with silane coupling agents during mixing at high temperatures, typically > 140°C. Silanization reaction leads to an increase in rubber–filler interaction, enhancing the mechanical and dynamical properties of rubber (3). On the other hand, the existing of low content silanol group from rice husk biosilica to the rubber compound generated low tensile properties and abrasion resistance of rubber as a result of weak rubber–filler interaction (9).

In this research, the usage of commercial biosilica containing high surface area and silanol groups in the formulation of energy-saving tread tire compound for passenger car tread tire compound was studied. The rubber compound formulation was designed, combining a blend of solution styrene-butadiene rubber (SSBR) and BR. This innovative blend was used with substantial quantities of both HD silica and biosilica, strategically incorporated to enhance the rubber compound. The effect of biosilica used to substitute HD silica was evaluated in detail, and various ratios between HD silica and biosilica were investigated. Subsequently, the Payne effect and rubber–filler interaction were analyzed to investigate the interaction between biosilica and rubber. Mechanical properties such as hardness and tensile properties were discussed, and the magic triangle properties of passenger car tread tire compound (i.e., abrasion resistance, wet grip, and rolling resistance) were also measured.

2 Materials and methods

2.1 Materials

SSBR Buna VSL 5025-0 HM and BR Nd-BR CB24 were purchased from Lanxess, Germany. SSBR/BR blend was strengthened by HD silica (Zeosil 1165 MP, Solvay, China), biosilica (Nano Powdering 550, Agrotech Industries, Indonesia), and Carbon Black N330 (OCI, Korea). TESPT (JHS69, Jianghan Fine Chemical Co. Ltd, China) was used to enhance the rubber–filler interaction. Naphthenic oil (Nytex 840, Nynas, Sweden) was used as a plasticizer. All compounds used *N*-cyclohexyl-2-benzothiazole sulfenamide (CBS OCP, Kemai Chemical Co. Ltd, China), diphenyl guanidine (DPG, Kemai Chemical Co. Ltd, China), and Tetrabenzylthiuram disulfide (Rhenogran TBzTd-70, Rhein Chemie Rheinau Mannheim GmbH, German) as accelerator. The compounds were protected against oxygen and ozone by using 2,2,4-trimethtyl-1,2-dihydroquinoline (TMQ Vulkanox HS/LG, Rhein Chemie Rheinau Mannheim GmbH, German), *p*-phenylenediamine (6PPD, Sirantox Vulkanox 4020, Lanxess, Deutschland GmbH, German), and wax (Antilux 654, Lanxess, Deutschland GmbH, German). Stearic acid (Aflux 52, Rhein Chemie Rheinau Mannheim GmbH, German) and zinc oxide (rubber activator, Lanxess, Deutschland GmbH, German) were used as an activator, and

sulfur (Midas SP-325, Miwon Chemicals Co., Ltd, Korea) was used as a vulcanizing agent.

2.2 Characterization of HD silica and biosilica

The characterization of silica and biosilica involved a comprehensive examination of their SSA and surface chemistry. The multipoint Brunauer–Emmet–Teller (BET) nitrogen surface area of HD silica and biosilica was determined according to ASTM D1993-18 standards. The BET test was performed using Quantachrome NOVA 4200e (Boynton Beach, Florida, USA). Subsequently, functional groups on HD silica and biosilica were investigated using attenuated total reflectance FTIR (ATR-FTIR) Nicolet iS5 (Thermo Scientific, USA). The samples HD silica and biosilica were dried at 105°C in an oven for 2 h and put in a desiccator before being characterized. The morphology of HD silica and biosilica were characterized using an Environmental scanning electron microscope (ESEM; Quattro, Thermo Fisher, USA). The samples without coating were directly tested in ESEM.

2.3 Preparation of passenger tread tire compound

Passenger car tread tire compound was prepared using the formulation shown in Table 1. The rubber compound was designed with different ratios between HD silica and biosilica while maintaining an equivalent number of total fillers of 80 parts per hundred rubber (phr). The ratios of HD silica/biosilica were varied at 80:0 (HD100), 60:20 (B25), 40:40 (B50), 20:60 (B75), and 0:80 (B100), respectively.

The mixing process was carried out using a Banbury mixer (David Bridge Co. Ltd, Manchester, England), following a three-stage mixing procedure as shown in Table 2. In the first stage, rubber materials were added with half of the silica, silane coupling agent, oil, activator, and protective agent. The mixer was operated at a fill factor of 70% and chamber temperature at 60°C with a rotor speed of 80 rpm. After all the materials were added into the Banbury mixer, the rotor speed was increased to 100 rpm, resulting in a chamber temperature rise to attain a dump temperature of 150°C, and this facilitated the execution of the silanization reaction (3). Subsequently, the dump temperature was measured and rubber compound was sheeted out using two roll mills to homogenous filler distribution and stored for 24 h at room temperature before being used for the next mixing stage.

In the second step, cold compound was re-mixed in the Banbury mixer. Initially, the chamber's temperature was calibrated to 60°C, accompanied by a rotor speed of 100 rpm, and a fill factor set at 70%. Subsequently, The silanization reaction was facilitated by the inclusion of DPG as an activator (11), and mixing persisted until the temperature reached 150°C. In the last mixing stage, accelerators and sulfur were added into the Banbury mixer with an initial temperature of 50°C and a fill factor of 65%. The compound was homogenized and sheeted out by using two roll mills, then stored at room temperature for 24 h.

Table 1: Passenger car tread tire compound formulations

Ingredients	Quantity (phr)				
	HD100	B25	B50	B75	B100
SSBR	75	75	75	75	75
BR	25	25	25	25	25
HD Silica, Zeosil 1165MP	80	60	40	20	0
Biosilica	0	20	40	60	80
Carbon black N330	5	5	5	5	5
TESPT	5.8	5.8	5.8	5.8	5.8
Naphthenic oil	26	26	26	26	26
ZnO	3	3	3	3	3
Stearic acid	2	2	2	2	2
TMQ	1.5	1.5	1.5	1.5	1.5
6PPD	2	2	2	2	2
Wax	2	2	2	2	2
DPG	2.5	2.5	2.5	2.5	2.5
CBS	1.6	1.6	1.6	1.6	1.6
TBZTD	0.2	0.2	0.2	0.2	0.2
Sulfur	2	2	2	2	2

Table 2: Mixing procedures

No.	Ingredients	Mixing time
	1st stage	
1.	SSBR dan BR	1 min
2.	½ silica + ½ silane + ½ oil	5 min
3.	½ silica + ½ silane + ½ oil + ZnO, stearic acid, TMQ, 6PPD	5 min
4.	Isothermal mixing at 140°C	
5.	Dump, check weight, sheet out, and storage 24 h	
	2nd stage	
1.	Add batch stage 1	1 min
2.	Add DPG	2 min
3.	Isothermal mixing at 140°C	
4.	Dump, check weight, sheet out, and storage 24 h	
	3rd stage	
1.	Add batch stage 2	1 min
2.	Add CBS, TBzTD, and sulfur	2 min
3.	Dump, check weight, sheet out, and storage 24 h	

2.4 Characterization of tread tire rubber compound

Filler–filler interaction which indicated the change in storage modulus (G′) at different strains of rubber compound without accelerator and the vulcanizing agent was analyzed by Rubber Processing Analyzer (RPA Elite, TA Instrument, USA). RPA was operated at 100°C, a frequency of 0.5 Hz under varying strains from 0.56% to 100%. The Payne effect was determined from G' at low and high strains, i.e., at 0.56% and 100%, respectively. The results from the first sweep were recorded.

Both the overall and chemically bound rubber contents were subjected to analysis. The physical linkages between rubber and silica were cleaved using ammonia, to determine chemical-bound rubber content (12). A total of 0.2 g rubber compound without curatives was cut into small pieces, put into a metal cage, and immersed in toluene with and without ammonia for 168 h. Furthermore, the samples were dried at 105°C for 24 h. The bound rubber contents were determined by the weights of samples before and after extraction using Eq. 1 as follows (12):

$$\text{Bound rubber content (\%)} = \frac{m - m_s}{m_r} \times 100 \quad (1)$$

where m is the weight of the sample after extraction, m_s is the weight of filler in the sample, and m_r is the weight of rubber in the sample.

The cure characteristics of tread tire compound with curatives agent were analyzed by using moving die rheometer (MDR 2000, Alpha Technology, USA) at 150°C to determine min torque (M_L), max torque (M_H), scorch time (t_s), and optimum curing time (t_{90}).

2.5 Morphology of tread tire vulcanizate

The dispersion of HD silica and biosilica in a rubber blend matrix was performed using ESEM. The cryogenic fractured surface of rubber vulcanizate was used as the testing specimens. The rubber vulcanizates HD100 and B100 were tested to show the influence of biosilica.

2.6 Characterization of tread tire rubber vulcanizate

The compound experienced were vulcanized, reaching the respective optimum cure time (t_{90}). This process was carried out using a laboratory compression press at 150°C and 100 kg·cm^{-2} in order to obtain vulcanized samples. To determine the apparent crosslink density, approximately 0.2 g of each vulcanized sample was immersed in 50 mL of aromatic solvent (toluene) for 72 h at room temperature. After immersion in toluene, the vulcanized sample was removed, blotted quickly with filter paper, weighed, and finally dried at room temperature for 24 h. The swelling value (Q) was identified as the number of grams of toluene absorption in rubber per gram of rubber hydrocarbon.

$$Q = \left(\frac{\text{Swollen weight} - \text{Dried weight}}{\text{Sample weight}}\right) \times \frac{\text{Formula Weight}}{100} \quad (2)$$

The formula weight is defined as the total weight of all compounding materials including rubber based on 100 phr. Apparent crosslink density was measured as reciprocal swelling value, $1/Q$ (13).

Tensile properties were tested using Universal Testing Machine (UTM; MTS, USA) operating at a crosshead speed of 500 mm·min^{-1} at room temperature according to ISO 37. The type 2 dumbbell specimens were prepared by die-cut of 2 mm thick vulcanized rubber. Three specimens were tested and the median value was recorded as the testing results.

Young's modulus was measured using UTM (MTS, USA) following the procedure outlined in ASTM E111-17. The measurement was carried out at room temperature, while the crosshead speed was set at 100 mm·min^{-1}. The specimens in accordance with dumbbell-shaped ISO 37 Type 2 were strained to 100% and then Young's modulus was calculated from the slope of the stress–strain curve at low strain (<100%). Three specimens were tested and the median value was recorded as the testing results. In addition, to evaluate the hardness of vulcanized rubber as per ISO 48–4, Shore A Frank Durometer was used.

Uniaxial cyclic testing was performed using UTM (MTS, USA) at a constant crosshead speed of 100 mm·min^{-1} at room temperature. The testing protocol employed dumbbell-shaped samples that were extracted from 2 mm thick plates, adhering to the specifications outlined in ISO 37 Type 2. The specimens were strained to 100% and four cycles were applied to obtain the hysteresis loop that was calculated by the ratio of areas under the loading and unloading curve, using Eq. 3 (14).

$$H = \frac{S_{load} - S_{unload}}{S_{load}} \quad (3)$$

where H is the hysteresis losses, and S_{load} and S_{unload} are areas under loading and unloading curves, respectively. In

addition, the softening stress was determined from the maximum stress value at the end of the loading path.

2.7 Magic triangle properties of tread tire rubber

The DIN volume loss was used to determine the abrasion resistance of rubber vulcanizate, performed by DIN Abrader according to the guidelines of ASTM D5963. Subsequently, three specimens were tested and the median value was recorded as the DIN volume loss for each sample.

The dynamic mechanical properties of rubber vulcanizate were characterized using Dynamic Mechanical Analyzer (DMA; DMA7100, Toshiba, Japan). The vulcanized rubber samples were cut into 20 mm × 9 mm × 2 mm specimens and tested in tension mode under temperature sweep between −80°C and 80°C at the frequency of 10 Hz and 0.1% strain. The heating rate during the test was determined at 2°C·min^{-1}. The tan δ at 0°C and 60°C was recorded indicating wet grip and rolling resistance of the tread tire, respectively.

Table 3: BET surface area, pore volume, and pore size of HD silica and biosilica

Samples	BET surface area ($m^2 \cdot g^{-1}$)	Pore volume ($cc \cdot g^{-1}$)	Pore size (nm)
HD Silica	130.5	0.0542	0.1838
Biosilica	124.6	0.0520	0.1838

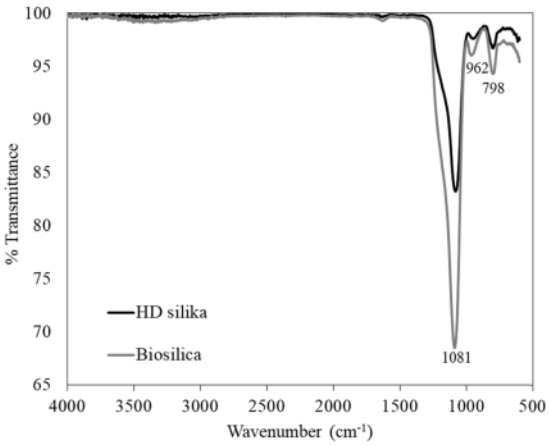

Figure 1: ATR-FTIR spectra of HD silica and biosilica.

3 Results

3.1 HD silica and biosilica properties

Silica serves as a filler primarily used to reinforce the rubber matrix. The properties of the reinforcing filler, such as surface area, structure, and surface activity parameters, significantly impact the mechanical and dynamic properties of elastomers (15). The surface area of silica is determined by using BET nitrogen adsorption, which indicated the total surface area including porosity (15). The multipoint BET surface area and pore volume of HD silica are slightly higher than biosilica as shown in Table 3. Furthermore, the Spectra ATR-FTIR and ESEM images of HD silica and biosilica are shown in Figures 1 and 2, respectively.

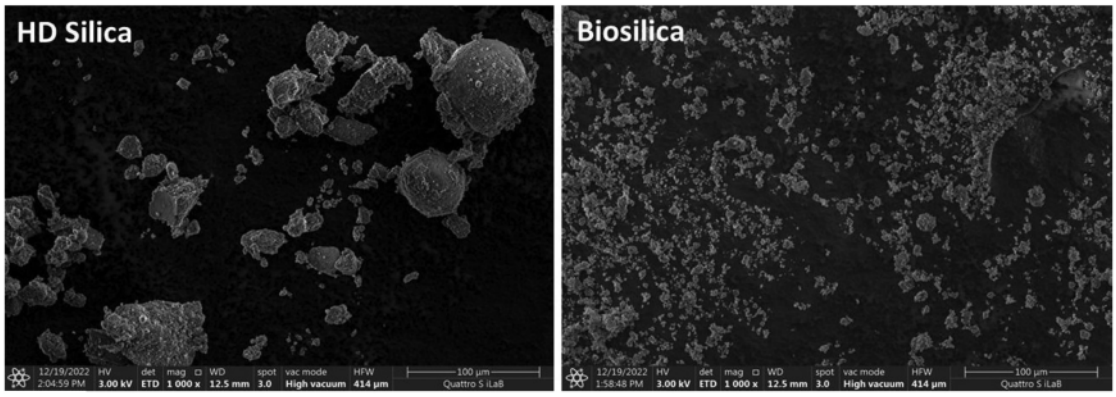

Figure 2: ESEM images (1,000× magnification) of HD silica and biosilica.

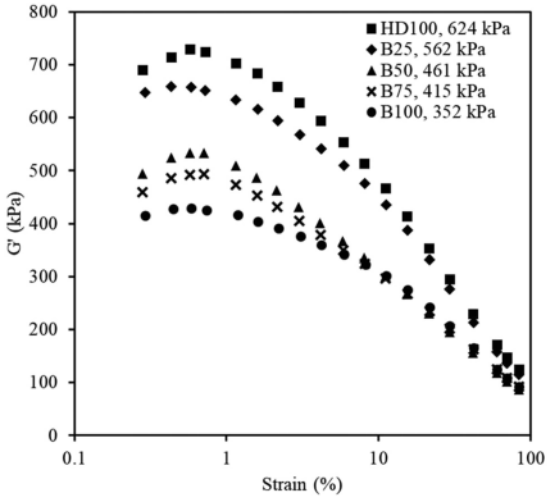

Figure 3: Storage modulus (*G'*) against strain of SSBR/BR-silica with different ratio of HD silica:biosilica compared to HD silica-filled SSBR/BR blend vulcanizate.

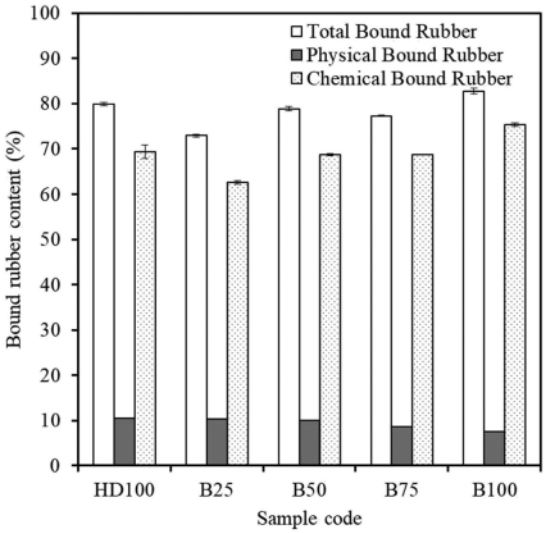

Figure 4: Total, physically, and chemically bound rubber contents of SSBR/BR-silica with different ratios of HD silica:biosilica compared to HD silica-filled SSBR/BR blend vulcanizate.

3.2 Properties of tread tire rubber compound

The investigation into the filler–filler interaction in silica-filled rubber, referred to as the "Payne effect," was conducted by observing the variation in storage modulus (*G'*) at different strain amplitudes. Figure 3 shows the strain dependence of *G'* at 100°C of rubber-HD silica compared to rubber-biosilica with different ratios of HD silica to biosilica.

The analysis of bound rubber content was used to determine the physical and chemical adsorption of silica onto SSBR/BR rubber blend, respectively. The total bound rubber indicates the physical and chemical interaction between rubber and reinforce filler. While the chemically bound rubber content was determined after applying ammonia treatment to cleavage the physical bonding between rubber and filler (12). Figure 4 shows the total physical and chemical bound rubber content of HD silica, biosilica, and HD silica/biosilica blend.

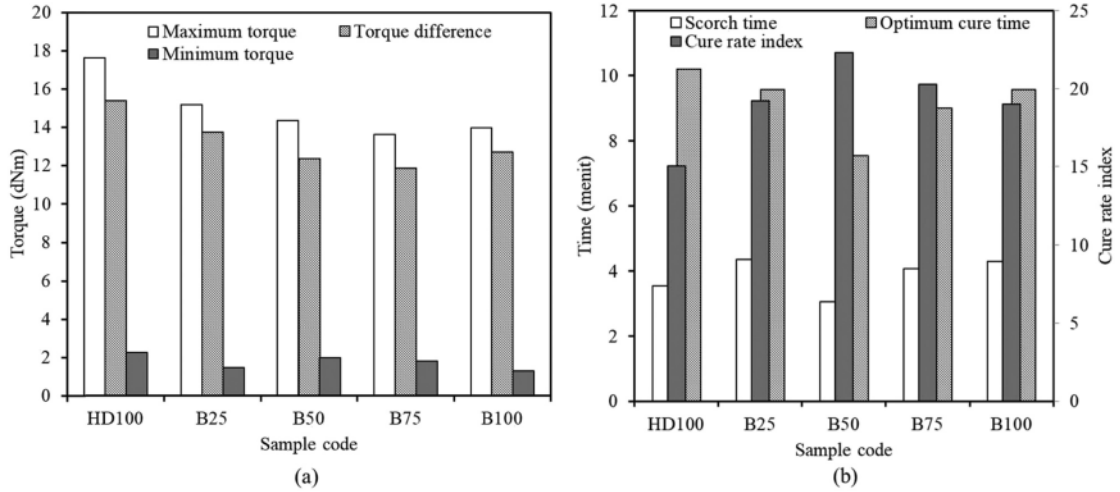

Figure 5: Cure torques (a), scorch time, cure time, and cure rate index (b) of SSBR/BR-silica with different ratios of HD silica:biosilica compared to HD silica-filled SSBR/BR blend vulcanizate.

The cure characteristics of HD silica, biosilica, and different ratios of HD silica/biosilica-filled rubber blend are shown in Figure 5.

3.3 Morphology of tread tire vulcanizate

The dispersion of HD silica and biosilica in tread tire vulcanizate captured by ESEM are shown in Figure 6.

3.4 Mechanical properties of tread tire rubber

The apparent crosslink density of HD silica, biosilica, and HD silica/biosilica blend filled in rubber blend vulcanizate is shown in Figure 7.

Figure 8 shows the modulus elasticity and hardness of HD silica, biosilica, and HD silica/biosilica blend filled in tread tire vulcanizate.

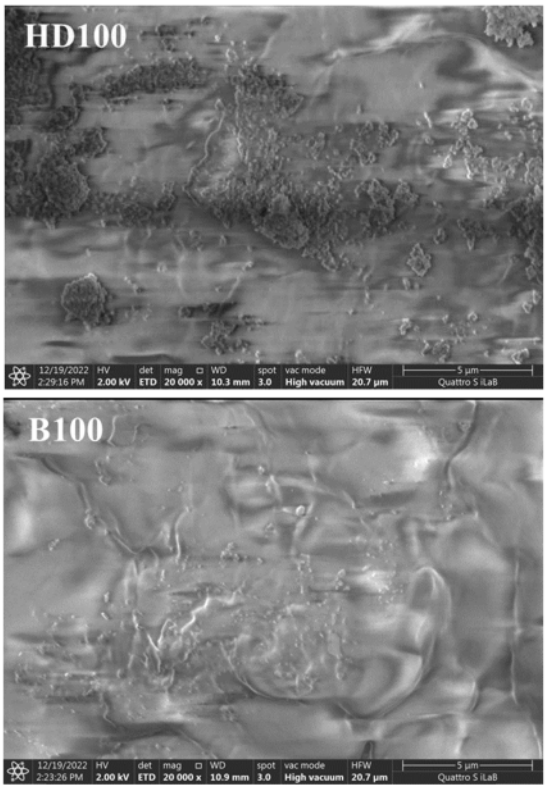

Figure 6: ESEM images (20,000× magnification) of biosilica compared to HD silica-filled SSBR/BR blend.

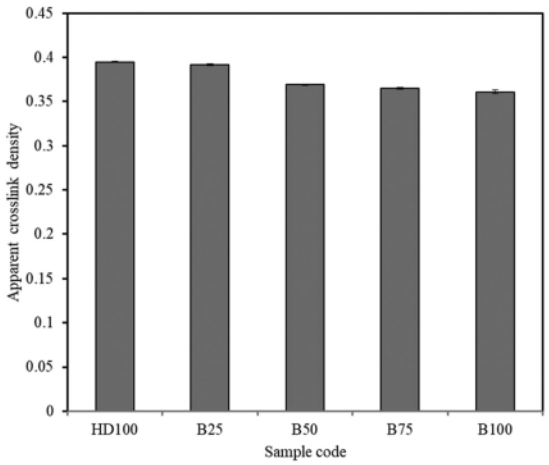

Figure 7: Apparent crosslink density of SSBR/BR-silica with different ratio of HD silica:biosilica compared to HD silica-filled SSBR/BR blend vulcanizate.

The tensile properties of biosilica and different ratios HD silica/biosilica filled rubber blend in terms of modulus 50% and 100% strain, tensile strength, and elongation at break of HD silica are shown in Figure 9.

The reinforcement phenomenon of silica-filled rubber was analyzed using stress softening (σ_{soft}), and behavior was determined by using the uniaxial cyclic test. Figure 10 shows the loading–unloading stress–strain curve for four cycles for HD silica, biosilica, and its blend filled in the rubber matrix.

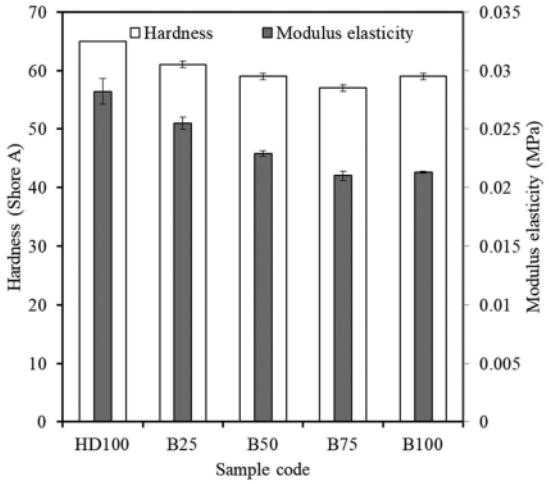

Figure 8: Modulus elasticity and hardness of SSBR/BR-silica with different ratios of HD silica:biosilica compared to HD silica-filled SSBR/BR blend vulcanizate.

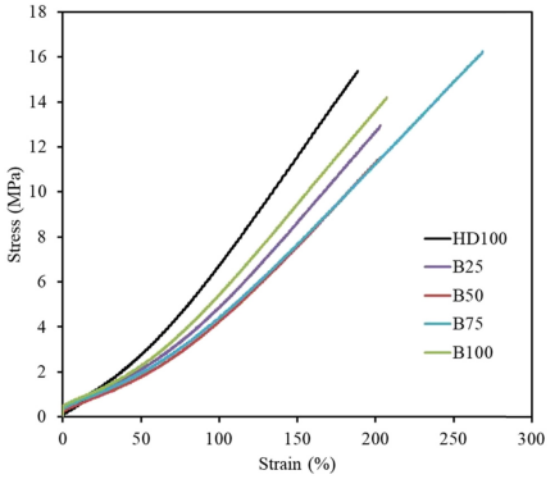

Figure 9: Stress–strain curve of SSBR/BR-silica with different ratios of HD silica:biosilica compared to HD silica-filled SSBR/BR blend vulcanizate.

The stress softening (σ_{soft}) values and hysteresis losses (H) are tabulated in Table 4.

3.5 Magic triangle properties of tread tire rubber

The incorporation of silica-silane-filled rubber enhances the characteristics of tread tire, leading to a reduction in rolling resistance, improved grip during braking, and maintained abrasion resistance (2). The abrasion resistance of tread rubber vulcanizate was determined using a DIN abrader. The DIN volume loss values are shown in Figure 11.

Loss tangent or tan δ as a function of the temperature of HD silica and biosilica with various ratios of biosilica-filled SSBR/BR blend are shown in Figure 12.

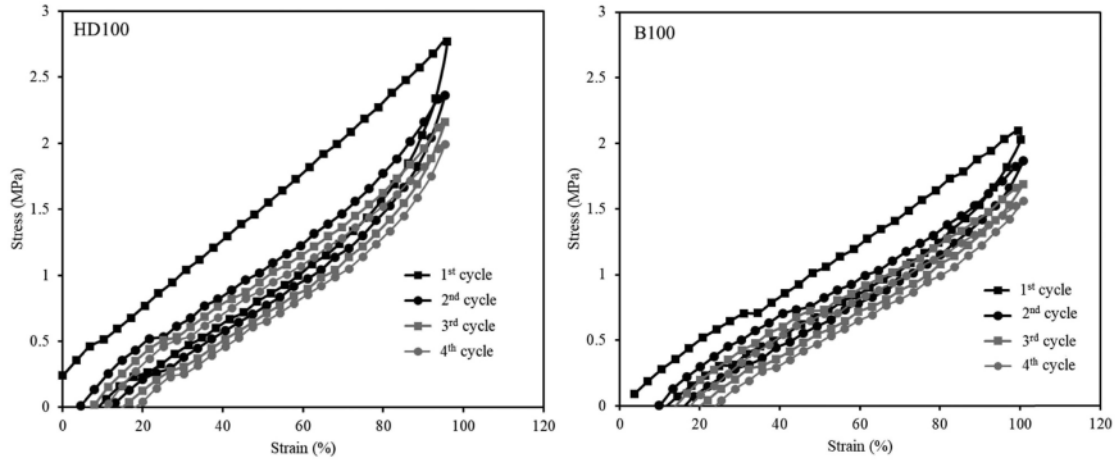

Figure 10: Four loading–unloading cycles of HD silica and biosilica-filled SSBR/BR blend vulcanizate.

Table 4: Stress softening of SSBR/BR-silica with different ratios of HD silica:biosilica compared to HD silica-filled SSBR/BR blend vulcanizate

Cycles	HD100		B25		B50		B75		B100	
	σ_{soft}	H	σ_{soft}	H	σ_{soft}	H	σ_{soft}	H	σ_{soft}	H
1	2.77	0.42	2.71	0.39	2.40	0.32	2.16	0.35	2.16	0.32
2	2.46	0.25	2.37	0.23	2.14	0.20	1.92	0.23	1.91	0.20
3	2.23	0.25	2.10	0.23	1.95	0.21	1.75	0.23	1.72	0.19
4	2.06	0.25	1.96	0.22	1.82	0.20	1.64	0.23	1.58	0.19

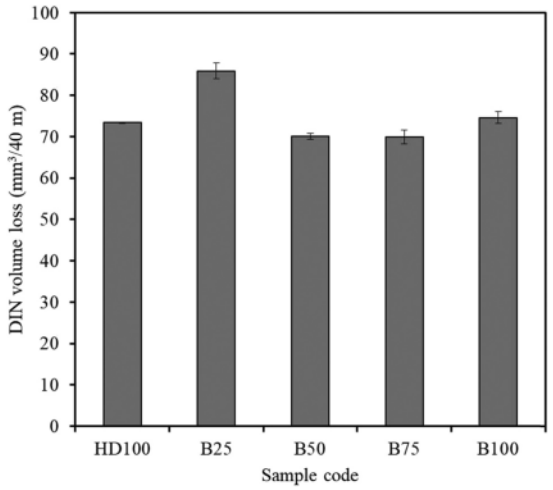

Figure 11: DIN volume loss of SSBR/BR-silica with different ratios of HD silica:biosilica compared to HD silica-filled SSBR/BR blend vulcanizate.

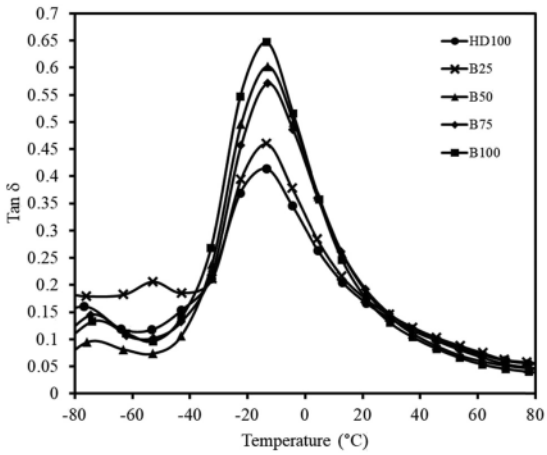

Figure 12: tan δ values against temperature of SSBR/BR-silica with different ratios of HD silica:biosilica compared to HD silica-filled SSBR/BR blend vulcanizate.

The wet grip and rolling resistance of tread tire vulcanizate could be predicted by DMA. The wet grip of tread tire vulcanizate was evaluated from tan δ value at 0°C. Meanwhile, rolling resistance was indicated from tan δ value at 60°C. Table 5 shows the wet grip and rolling resistance of tread tire vulcanizate with different HD silica:biosilica ratios.

4 Discussion

4.1 HD silica and biosilica properties

As shown in Table 3, the elevation in BET surface area is directly attributed to the corresponding augmentation in silica's pore volume (16). Higher BET surface area and pore volume contribute to better incorporation of silica in rubber matrix (5).

The result of ATR-FTIR analysis shows striking similarities between the spectra of HD silica and biosilica. The highest peak is shown at a wavenumber of 1,081 cm^{-1} for HD silica and 1,089 cm^{-1} for biosilica assigned symmetric stretching vibration of Si–O on Si–O–Si, respectively. In addition, the spectra ATR-FTIR of HD silica and biosilica show symmetric stretching vibration of Si–O on Si–O–Si at wavenumber 799 cm^{-1} (6,10). These particular peaks are considered as the main peaks for silica materials (17). However, some silica materials show different peak at wavenumber 963 cm^{-1} which indicates asymmetric stretching vibration of Si–O on Si–OH (10,17). Interestingly, ATR-FTIR spectra of both silica do not show O–H stretching and O–H bending at a broad peak of 3,200–3,600 and 1,650 cm^{-1}, respectively. This indicates the absence of water molecules in silica particles (18). During preparation, before use in the rubber compound, HD silica and biosilica were dried at 105°C for 4 h. Consequently, any water molecules present within the silica particles evaporated during this drying procedure.

The morphology of both silica shows irregular shapes. However, the morphology of HD silica shows the presence of certain spherical agglomerations. The size of agglomerate biosilica particles is smaller compared to HD silica. The presence of silanol groups on silica surfaces as shown in the ATR-FTIR result (Figure 1) leads to the formation of aggregates or agglomerates between silica particles due to hydrogen bonding interaction (1).

4.2 Properties of tread tire rubber compound

Figure 3 shows the Payne effect value derived from the calculation of the difference between G' (storage modulus)

Table 5: Wet grip and rolling resistance of SSBR/BR-silica with different ratios of HD silica:biosilica compared to HD silica-filled SSBR/BR blend vulcanizate

Parameters	Samples code				
	K100	B25	B50	B75	B100
tan δ at 0°C	0.306	0.336	0.441	0.425	0.441
tan δ at 60°C	0.074	0.078	0.061	0.070	0.055

at 100% strain and G' at 0.56% strain. The Payne effect of HD silica-filled rubber blend is higher compared to biosilica-filled rubber blend uncured compound. The addition of biosilica into tread tire compound decreased the Payne effect and G' at low strain value because a higher BET surface area of HD silica can promote the aggregation of silica particles (16). Furthermore, the incorporation of biosilica serves to decrease the interactions between fillers within tread tire compound. This observation suggests that TESPT (tetrasulfide silane) demonstrates effective interaction with silica surfaces, thereby enhancing the hydrophobic characteristics of the silica component, and providing better compatibility between silica and SSBR/BR blend. In this research, the same amount of TESPT was used in tread tire compound formulation. However, it is important to note that the amount of TESPT depended on the SSA of silica (19). Therefore, biosilica compound contains slightly higher TESPT which can enhance rubber–filler interaction and reduce filler–filler interaction of silica.

HD silica-filled rubber blend compound shows slightly higher physically bound rubber content. Meanwhile, the addition of biosilica leads to a reduction in the physical interaction between rubber and filler. This phenomenon is confirmed by the Payne effect result as shown in Figure 3. The physical interaction between rubber and silica is not only due to the interaction between silica particles but also the physical adsorption of rubber onto silica particles in the presence of a silane coupling agent. HD silica with higher BET surface area and pore volume facilitates the absorption of TESPT onto the silica surface. Furthermore, rubber chains are adsorbed to the silica surfaces to form stable and unstable interactions between rubber and silica (20).

The chemically bound rubber content of biosilica is higher than HD silica-filled rubber blend compound. However, when examining rubber compound with varying ratios of HD silica and biosilica, the chemically bound rubber content appears to be relatively comparable across different formulations. The chemically bound rubber content denotes chemical interaction among rubber, TESPT, and silica. Lower agglomeration of biosilica as shown in the Payne effect value (Figure 3) of biosilica-filled rubber blend supports better interaction among rubber, TESPT, and silica. Moreover, a slightly higher amount of TESPT based on the SSA in biosilica leads to an initiated silanization reaction and increases chemical-bound rubber content.

Among the various rubber blends, those containing HD silica exhibit the most notable values for minimum, maximum, and torque differences. However, the incorporation of biosilica into tread tire compound results in a reduction in M_H (maximum torque), M_L (minimum torque), and the torque difference (M_H–M_L). In general, a decrease in M_L leads to a reduction in viscosity and indicates better processing due to an increased degree of silanization reaction between rubber and silica as a consequence of better Payne effect as shown in Figure 3. The decreasing M_H and torque difference (M_H–M_L) due to the decreasing Payne effect value and increasing chemical bound rubber are shown in Figure 4.

The scorch time of HD silica, biosilica, and HD silica/biosilica blend are comparable. Meanwhile, distinct variations become evident in terms of the optimal cure time and the cure rate index, and lower optimum time and higher cure rate index indicate better productivity. It can be seen that the cure rate index of HD silica-filled rubber blend is lower than biosilica in tread tire compound. The presence of acid silanol groups causes the adsorption of base accelerators on silica surfaces, and as a result, it inhibits the vulcanization reaction (21). As previously mentioned, the amount of TESPT depends on the SSA of silica. Therefore, higher SSA increase TESPT doses in rubber compound. This research is in line with the work reported by Lolage et al. (5), the compound containing rice husk silica showed a lower cure time and higher cure rate index.

4.3 Morphology of tread tire vulcanizate

As shown in Figure 6, distinct aggregates and agglomerates of HD silica are prominently showcased. The formation of aggregates and agglomerates of HD silica due to the interaction between HD silica is due to the hydrogen bonding between silanol groups on the HD silica surfaces. This mechanism contributes to the formation of a filler network, leading to an augmentation of the Payne effect value, as corroborated by the observations presented in Figure 3. On the other hand, the dispersion of biosilica in the SSBR/BR blend matrix is better than HD100 tread tire vulcanizate samples as shown in Figure 6. This result is in line with the Payne effect results (Figure 3).

4.4 Mechanical properties of tread tire rubber

The observed crosslink density shows a slight reduction as the proportion of biosilica in tread tire vulcanizate increases. This apparent crosslink density was assessed through the swelling technique in toluene. The filler containing rubber vulcanizate retards the adsorption of toluene, and the higher filler-filler interaction tends to increase trapped rubber (1). Therefore, some rubber molecules are unable to come in

contact with toluene, leading to a decrease in swelling value. However, the addition of biosilica decreases the Payne effect as shown in Figure 3. The reduction of the Payne effect induces more contact between rubber and toluene, and this affects the increasing swelling value and decreasing apparent crosslink density, respectively.

Modulus elasticity (Young's modulus) and hardness of HD silica-filled rubber blend vulcanizate show the highest values. The hardness of rubber is correlated to Young's modulus by theoretical and empirical equations (22). The relationship is determined at low strain using UTM. At this condition, the reinforcement effect is due to the formation of a filler network (23). Therefore, the increase in Young's modulus and hardness resulted from the increase in the Payne effect value of high-dispersion silica within tread tire compound. On the contrary, the addition of biosilica tends to decrease the Payne effect, Young's modulus, and hardness of tread tire, respectively.

As shown in Figure 9, the HD silica-filled rubber (HD100) curve has higher stress compared to biosilica-filled rubber at the same strain. Furthermore, more biosilica loading in rubber matrix tends to reduce stress. However, the biosilica-filled SSBR/BR blend (B100) shows the opposite direction since it has the highest stress than other HD silica/biosilica-filled rubber blend. This enhanced performance can be attributed to the prevalence of rubber–filler interaction, particularly evident through bound rubber, during low-strain conditions of either 50% or 100%. This dominance surpasses the filler–filler (Payne effect) or rubber–rubber (crosslink density) interactions. Therefore, stress at a low strain of biosilica-filled SSBR/BR blend is more influenced by rubber–filler interaction.

The incorporation of biosilica into the rubber matrix leads to a slight reduction in tensile strength while resulting in an increase in elongation at break. This indicates that at high strain, filler networks break down and rearrange. Stress is mainly contributed by chemical rubber–filler interaction and rubber network (23). The lower the filler network, the larger the inter-aggregate distance of biosilica leading to the mobility of the chains, which is not restricted by filler. As a consequence, it resulted in increasing elongation at break but decreased tensile strength properties.

The occurrence of stress-softening behavior (Mullins and Tobin effect) is evident in all vulcanizate samples. Stress softening and hysteresis loss are more pronounced at the first to second stretching, and further softening is very weak. This phenomenon is due to many aspects, i.e., the breaking of filler networks, agglomerates, aggregates, rubber–filler linkages, or slippage of the elastomer chains at the filler surface (24). During the first hysteresis area, filler network and/or rubber–filler linkages breakdown caused the formation of dissipated energy. The higher Payne effect value of HD silica in tread tire compound is accompanied by increased hysteresis losses. The addition of biosilica suppressed the filler network and caused the decrease in the hysteresis losses.

4.5 Magic triangle properties of tread tire rubber

The lower DIN volume loss values result in better abrasion resistance. The abrasion resistance of HD silica is comparable to B50, B75, and B100 tread tire vulcanizate, and highly influenced by filler–rubber interaction and crosslink density (25). The addition of biosilica led to enhance chemically bonded rubber and a reduced silica network due to the better interaction between TESPT and silanol groups on silica surfaces.

The tan δ at the peak of HD silica-filled SSBR/BR blend vulcanizate is lower than biosilica-filled SSBR/BR blend vulcanizate. This indicates that the filler network of the HD silica-based compound is stronger, consistent with its elevated Payne effect value (Figure 3). In the glassy regions, the main contribution of energy dissipation is the rubber matrix. The higher filler network leads to entrapping the rubber chains in the filler networks. Therefore, the ratio of rubber in the compound will reduce since the filler network cannot be easily broken causing the decrease in the tan δ at peak (1,26). The presence of biosilica decreases the filler network as shown in Figure 3. Moreover, increasing the chain mobility of rubber and loose rubber chains contribute to energy loss resulting in increased tan δ at the peak.

The improved wet grip of tread tire is accompanied by a higher tan δ value at 0°C. It is important to note that the inclusion of biosilica in tread tire compound enhances wet grip. The addition of 100% biosilica (B100) to substitute HD silica results in the highest tan δ value at 0°C. This phenomenon describes that better dispersion of silica leads to an increase in the chain mobility of rubber and results in increasing tan δ at 0°C. The lower value of tan δ at 60°C shows better rolling resistance. The filler network will break down due to the increase in temperature, and the main contribution of energy dissipation is affected by the rubber network and chemical interaction between rubber and filler. For the HD 100 and B25 tread tire vulcanizates with higher Payne effect values, the filler network is broken during testing. As the temperature rises, the rubber chains previously trapped within filler clusters are released, leading to an elevated tan δ value at 60°C, which indicates an unfavorable impact on rolling resistance. Meanwhile,

with an increased quantity of biosilica (B50, B75, and B100), the tan δ value at 60°C decreases, signifying an improvement in rolling resistance. This is due to the increasing filler dispersion and chemically bound rubber of biosilica-filled SSBR/BR blend as shown in Figures 3 and 4, respectively. Therefore, based on the performance of tread tire vulcanizate testing, HD silica can be substituted by biosilica for a minimum ratio of HD silica: biosilica (50:50) to enhance wet grip and rolling resistance while maintaining the abrasion resistance.

5 Conclusion

In conclusion, this research focused on the integration of biosilica into energy-saving tire compound composed of SSBR/BR blend, serving as a substitute for HD silica. The BET surface area of biosilica was slightly lower than HD silica but exhibited similar functional groups, including silanol groups and silicon, as confirmed by ATR-FTIR analysis. The dispersion of biosilica in SSBR/BR blend was confirmed by RPA and ESEM which showed that the addition of biosilica into the SSBR/BR matrix improved silica dispersion, compared to HD silica tire compound. The introduction of biosilica into the SSBR/BR matrix led to the suppression of the filler network, resulting in reduced minimum torque and enhanced vulcanization reaction. However, there was a slight decrease in hardness, Young's modulus, and tensile strength as the amount of biosilica filled increased in the SSBR/BR blend. In addition, hysteresis loss of biosilica was lower than HD silica filled in SSBR/BR blend, consistent with tan δ value at 60°C. In the context of the magic triangle of tread tire properties, the incorporation of biosilica led to improved wet grip and rolling resistance while maintaining abrasion resistance.

Acknowledgements: The authors are grateful to the Head of the Bogor Getas Research Unit for providing facilities to conduct this research project. The authors are also grateful to Mr. Aos Kosasih, Mr. Jaenal, Ms. Woro Andriani, and Ms. Selviani (Research Technician, Bogor Getas Research Unit) for their support during the experiment and observation. Furthermore, the authors are grateful to Mr. Ahmad Syarif Hidayatulloh, Mr. Reyhan Avdhinal Aldilfli, and Mr. Muktar Mulyani (Laboratory Analyst, Bogor Getas Research Unit) for the contribution to the analysis and testing work during the research project.

Funding information: This research project funding was supported by the National Research and Innovation Agency and Indonesia Endowment Fund for Education through Research Innovation for Advanced Indonesia Batch 2, 2022 with contract number 86/IV/KS/11/2022.

Author contributions: Mohamad Irfan Fathurrohman: project supervisor, conceptualization, methodology, investigation, formal analysis, and writing – original draft; Santi Puspitasari: data curation, investigation, formal analysis, writing – review and editing, and manuscript handling; Asron Ferdian Falaah: investigation, data curation, and formal analysis; Lydia Anggraini: conceptualization, investigation, and writing – review and editing; Nanang Ali Sutisna: methodology, investigation, formal analysis, and writing – review and editing; Rijal Hakiki: investigation and data curation.

Conflict of interest: The authors state no conflict of interest.

Data availability statement: The raw and processed data generated and analyzed that support the findings of this current research project are available from the corresponding author [MIF], upon reasonable request.

References

(1) Wang MJ. The role of filler networking in dynamic properties of filled rubber. Rubber Chem Technol. 1999;72(2):430–48. doi: 10.5254/1.3538812.
(2) Wolff S. Silanes in tire compounding after ten years – a review. Tire Sci Technol. 1987;15(4):276–94. doi: 10.2346/1.2148794.
(3) Brinke JWT, Debnath SC, Reuvekamp LAEM, Noordermeer JWM. Mechanistic aspects of the role of coupling agents in silica–rubber composites. Compos Sci Technol. 2003;63(8):1165–74. doi: 10.1016/S0266-3538(03)00077-0.
(4) Paul SC, Mbewe PB, Kong SY, Savija B. Agricultural solid waste as source of supplementary cementitious materials in developing countries. Mater. 2019;12(7):1112. doi: 10.3390/ma12071112.
(5) Lolage M, Parida P, Chaskar M, Gupta A, Rautaray D. Green silica: industrially scalable & sustainable approach towards achieving improved "nano filler–elastomer" interaction and reinforcement in tire tread compounds. Sustainable Mater Technol. 2020;26:e00232. doi: 10.1016/j.susmat.2020.e00232.
(6) Chundawat NS, Parmar BS, Deuri AS, Vaidya D, Jadoun S, Zarrintaj P, et al. Rice husk silica as a sustainable filler in the tire industry. Arabian J Chem. 2022;15(9):104086. doi: 10.1016/j.arabjc.2022.104086.
(7) Steven S, Restiawaty E, Bindar Y. Routes for energy and bio-silica production from rice husk: A comprehensive review and emerging prospect. Renewable Sustainable Energy Rev. 2021;149:111329. doi: 10.1016/j.rser.2021.111329.
(8) Arayapranee W, Na-Ranong N, Rempel GL. Application of rice husk ash as fillers in the natural rubber industry. J Appl Polym Sci. 2005;98(1):34–41. doi: 10.1002/app.21004.

(9) Sae-Oui P, Rakdee C, Thanmathorn P. Use of rice husk ash as filler in natural rubber vulcanizates: In comparison with other commercial fillers. J Appl Polym Sci. 2002;83(11):2485–93. doi: 10.1002/app.10249.
(10) Mujiyanti DR, Ariyani D, Lisa M. Silica content analysis of siam unus rice husks from South Kalimantan. Indonesian J Chem Res. 2021;9(2):81–7. doi: 10.30598//ijcr.2020.9-muj.
(11) Kaewsakul W, Sahakaro K, Dierkes WK, Noordermeer JWM. Optimization of mixing conditions for silica-reinforced natural rubber tire tread compounds. Rubber Chem Technol. 2012;85(2):277–94. doi: 10.5254/rct.12.88935.
(12) Wolff S, Wang MJ, Tan EH. Filler-elastomer interactions. Part VII. Study on bound rubber. Rubber Chem Technol. 1993;66(2):163–77. doi: 10.5254/1.3538304.
(13) Sarkawi SS, Dierkes WK, Noordermeer JWM. Elucidation of filler-to-filler and filler-to-rubber interactions in silica-reinforced natural rubber by TEM Network Visualization. Eur Polym J. 2014;54:118–27. doi: 10.1016/j.eurpolymj.2014.02.015.
(14) Starkova O, Aniskevich A. Softening of silica filled styrene-butadiene rubber under uniaxial cyclic loading. Mater Sci. 2016;22(2):273–8. doi: 10.5755/j01.ms.22.2.7953.
(15) Niedermeier W, Frohlich J, Luginsland H. Reinforcement mechanism in the rubber matrix by active fillers. Kautsch Gummi Kunstst. 2002;55(7–8):356–66.
(16) Ryu C, Kim SJ, Kim DI, Kaang S, Seo G. The effect of surface area of Silicas on their reinforcing performance to styrene-butadiene rubber compounds. Elastomers Compos. 2016;51(2):128–37. doi: 10.7473/EC.2016.51.2.128.
(17) Boonmee A, Sabsiriroht P, Jarukumjorn K. Preparation and characterization of rice husk ash for using as a filler in natural rubber. Mater Today Proc. 2019;17:2097–103. doi: 10.1016/j.matpr.2019.06.259.
(18) Choophun N, Chaiammart N, Sukthavon K, Veranitisagul C, Laobuthee A, Watthanaphanit A, et al. Natural rubber composites reinforced with green silica from rice husk: effect of filler loading on mechanical properties. J Compos Sci. 2022;6(12):369. doi: 10.3390/jcs6120369.
(19) Guy L, Daudey S, Cochet P, Bomal Y. New insights in the dynamic properties of precipitated silica filled rubber using a new high surface silica. Kautsch Gummi Kunstst. 2009;62(7-8):383–91.
(20) Clement F, Bokobza L, Monnerie L. Investigation of the Payne effect and its temperature dependence on silica-filled polydimethylsiloxane networks. Part I: Experimental results. Rubber Chem Technol. 2005;78(2):211–31. doi: 10.5254/1.3547879.
(21) Qian Z, Peng Z. Reinforcing styrene-butadiene rubber composites by constructing multiple interaction between rubber and silica. Polym Compos. 2019;40(5):1740–7. doi: 10.1002/pc.24928.
(22) Murali Manohar D, Chakraborty BC, Shamshath Begum S. Hardness–elastic modulus relationship for nitrile rubber and nitrile rubber–polyvinyl chloride blends. In: Ganippa L, Karthikeyan R, Muralidharan V, editors. Adv Des Ther Syst. Singapore: Springer; 2021. p. 301–14. doi: 10.1007/978-981-33-6428-8_24.
(23) Sahakaro K. Mechanism of reinforcement using nanofillers in rubber nanocomposites. In: Thomas S, Maria HJ, editors. Prog Rubber Nanocomposites. Cambridge, UK: Woodhead Publishing; 2017. p. 81–113.
(24) Bokobza L. The reinforcement of elastomeric networks by fillers. Macromol Mater Eng. 2004;289(7):607–21. doi: 10.1002/mame.200400034.
(25) Wang MJ. Effect of filler-elastomer interaction on tire tread performance part III effects on abrasion. Kautsch Gummi Kunstst. 2008;61(4):159–65.
(26) Li Y, Han B, Liu L, Zhang F, Zhang L, Wen S, et al. Surface modification of silica by two-step method and properties of solution styrene butadiene rubber (SSBR) nanocomposites filled with modified silica. Compos Sci Technol. 2013;88:69–75. doi: 10.1016/j.compscitech.2013.08.029.

Turnitin artikel bu Lidya

ORIGINALITY REPORT

4%	6%	7%	1%
SIMILARITY INDEX	INTERNET SOURCES	PUBLICATIONS	STUDENT PAPERS

MATCH ALL SOURCES (ONLY SELECTED SOURCE PRINTED)

1%

★ hdl.handle.net

Internet Source

Exclude quotes	On	Exclude matches	< 1%
Exclude bibliography	On		